J Pharmacol Sci **124**, 445 – 456 (2014)

Journal of Pharmacological Sciences
© The Japanese Pharmacological Society

Full Paper

Effect of *Sedum sarmentosum* Bunge Extract on Aristolochic Acid–Induced Renal Tubular Epithelial Cell Injury

Yongheng Bai[1], Hong Lu[2], Liping Hu[2], Dan Hong[3], Linchao Ding[3], and Bicheng Chen[1,*]

[1]*Wenzhou Key Laboratory of Surgery,* [2]*Department of Laboratory Medicine, The First Affiliated Hospital, Wenzhou Medical University, Wenzhou 325000, China*
[3]*School of Laboratory Medicine and Life Science, Wenzhou Medical University, Wenzhou 325035, China*

Received October 25, 2013; Accepted February 2, 2014

Abstract. Aristolochic acid (AA) is known as a potent mutagen that induces significant cytotoxic and mutagenic effects on renal tubular epithelial cells. Clinically, the persistent injury of AA results in the infiltration of inflammatory cells, epithelial-to-mesenchymal transition (EMT), and renal tubulointerstitial fibrosis. There are no truly effective pharmaceuticals. In this study, we investigated the potential role of the extract of *Sedum sarmentosum* Bunge (SSB), a traditional Chinese herbal medicine, on rat tubuloepithelial (NRK-52E) cells after AA injury in vitro. Evidence revealed that AA induced mitochondrial-pathway–mediated cellular apoptosis, accompanied by cell proliferation in a feedback mechanism. Treatment with SSB also induced cells to enter early apoptosis, but inhibited cell proliferation. In cultured NRK-52E cells, AA induced the imbalance of MMP-2/TIMP-2 and promoted EMT and ECM accumulation. SSB treatment significantly alleviated AA-induced NRK-52E cells fibrosis-like appearance, inhibited the induction of EMT, and deposition of ECM. SSB also decreased the activity of the NF-κB signaling pathway, resulting in down-regulated expression of NF-κB–controlled chemokines and pro-inflammatory cytokines, including MCP-1, MIF, and M-CSF, which may regulate the macrophage-mediated inflammatory reaction during renal fibrosis in vivo. Therefore, these findings suggest that SSB exerts protective effects against AA-induced tubular epithelial cells injury through suppressing the synthesis of inflammatory factors, EMT, and ECM production.

Keywords: aristolochic acid, epithelial-to-mesenchymal transition, renal fibrosis, *Sedum sarmentosum* Bunge, inflammation

Introduction

Aristolochic acid nephropathy (AAN) is a devastating disease leading to chronic renal failure and urothelial cancers (1 – 3). Many patients have to undergo long-term hemodialysis and kidney transplantation due to rapid and irreparable kidney impairment. Although aristolochic acid (AA) in several traditional herbal preparations has been shown to cause progressive renal failure, many people in Asian countries such as China and Japan (4 – 6) still used these preparations without a doctor's prescription or guidance. Therefore, further studies are needed to investigate AA's potential pathogenesis and effective cures to avoid progressive kidney damage.

Clinically, the histopathology of AAN features interstitial matrix deposition in association with inflammatory cells, tubular cell loss, fibroblast accumulation, and rarefaction of the peritubular microvasculature (7). As to kidney tissues, the persistent injury of AA will markedly alter the micro-environment and induce the infiltration of inflammatory cells, cellular apoptosis and necrosis, the transition from epithelial cells to mesenchymal cells (EMT), and nonparenchymal cell proliferation, gradually damaging the normal structure of the kidney. As a result, the functional nephrons are markedly reduced and injured tubular epithelial cells (RTECs) will be replaced by proliferating fibroblast cells, extracellular matrix (ECM) deposition, and inflammatory cells. Major epithe-

*Corresponding author. greatsailor@163.com
Published online in J-STAGE on March 27, 2014
doi: 10.1254/jphs.13216FP

lial mechanisms contributing to interstitial fibrosis after AA injury are G2/M cell cycle arrest, cellular apoptosis, and EMT-forming fibroblasts (8 – 10). G2/M arrest activates c-jun NH_2-terminal kinase signaling, resulting in up-regulated expression of profibrotic gene transforming growth factor-β1 (TGF-β1) in vitro and collagen production in vivo. In addition, in AA-treated RTECs, enhanced TGF-β1 expression promotes EMT, which is reversed by bone morphogenic protein-7 (BMP-7) (11, 12). Furthermore, during interstitial fibrosis, many chemokines (e.g., monocyte chemoattractant protein-1, MCP-1) and pro-inflammatory cytokines (e.g., macrophage migration inhibitory factor, MIF) expressed in RTECs are involved in the inflammatory reaction by activating the nuclear factor-kappa B (NF-κB) pathway (13 – 15). Thus, effective therapeutic cures should include reduction of the inflammatory reaction, inhibition of EMT, and deposition of ECM.

Sedum sarmentosum Bunge (SSB) is a perennial herb widely distributed on the mountain slopes in Asian countries and traditionally used for the treatment of some inflammatory diseases (16 – 18). SSB contains multiple active chemical components, including tricin-7-*O*-β-D-glucoside, isorhamnetin, quercetin, and kaempferide (19 – 21). Isorhamnetin is an *O*-methylated flavonol, a type of chemical compound that has biological activity such as anti-oxidant, anti-cancer, and improvement of cardiovascular function (22). Quercetin is a plant-derived flavonoid that has the potential antiviral (23), anti-cancer (24, 25), and anti-inflammatory properties (26). These active components endow SSB with many kinds of pharmacological activity, including anti-inflammatory action. Considering that inflammation and oxidation are critical pathogenic factors in fibrogenesis, it is hypothesized that SSB is capable of anti-renal fibrosis action.

However, a study on the role of the anti-fibrosis effect of SSB in AAN has not been performed. Therefore, for the first time, we investigated the effects of SSB on AA-induced RTECs injury in vitro by evaluating cellular proliferation and apoptosis, EMT, and the accumulation of ECM components. Furthermore, we also examined the expression levels of chemokines and pro-inflammatory cytokines in cultured RTECs, evaluating the involvement of the NF-κB signaling pathway.

Materials and Methods

Cell culture and treatment

The normal rat kidney tubule epithelium (NRK-52E) cell line was obtained from the Cell Bank of Chinese Academy of Sciences (Shanghai, China). NRK-52E cells were maintained in Dulbecco's Modified Eagle Medium (Invitrogen, Carlsbad, CA, USA) supplemented with 5% fetal bovine serum (FBS, Invitrogen), 100 U/ml penicillin, and 100 μg/ml streptomycin (Invitrogen). The NRK-52E cells were seeded on six-well culture plates to approximately 70% confluence in the complete medium containing 5% FBS for 24 h and then changed to serum-free medium for 24 h before the treatment with aristolochic acid I (lot No. A5512; Sigma-Aldrich, St. Louis, MO, USA) or *Sedum sarmentosum* Bunge (SSB, lot No. 20101017, Xuancheng Baicao Plant Industry and Trade Co., Ltd., Anhui, China). The extraction protocol of SSB is shown in Fig. 1.

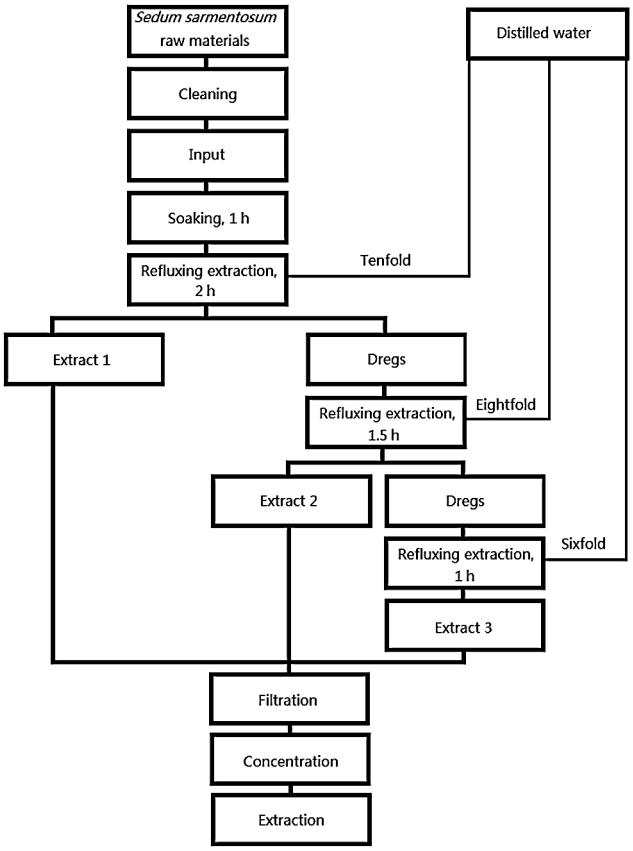


Fig. 1. The extraction protocol of *Sedum sarmentosum* Bunge.

Cell viability assay

Viability of NRK-52E cells treated with AA alone or in combination with SSB was measured using the Water Soluble Tetrazolium Salt (WST-1) Cell Proliferation and Cytotoxicity Assay kit (Beyotime Biotechnology, Jiangsu, China) according to the manufacturer's instructions. At the indicated time points, 10 μl of this reagent at different concentrations was added to each well containing 100 μl of cell suspension (5×10^3 cells) and incubated for an additional 1 h. The absorbance at 450 nm was monitored and the reference wavelength was

set to 690 nm. The percent viability of cells was calculated by comparison to that of untreated control cells.

Apoptosis assay

Cells treated with AA and/or SSB were seeded for 24 h on sterile cover glasses placed in the six-well plates and then fixed, washed twice with phosphate-buffered saline (PBS), and stained with Hoechst 33258 and Propidium staining solution in accordance with the manufacturer's instructions (Beyotime Biotechnology). Stained nuclei were observed and pictures were taken using a DM4000 B LED Microscope System (Leica Microsystems, Wetzlar, Germany) and DFC 420 C 5M Digital Microscope Camera (Leica).

Immunofluorescence staining

NRK-52E cells were cultured with AA and/or SSB on six-well plates containing glass slides,washed in PBS, and then fixed in 4% paraformaldehyde (Sigma-Aldrich) at 4°C for 30 min. After permeabilization in 0.1% Triton X-100 for 10 min, specimens were washed in PBS, and then treated with 10% FBS prior to incubation with the primary antibody to eliminate the nonspecific fluorescence. Immunofluorescence staining was performed using anti-type III collagen (1:100; Biogot Technology, Shanghai, China), α-SMA (1:200; Santa Cruz Biotechnology, Santa Cruz, CA, USA), MIF (1:200, Santa Cruz), MCP-1 (1:100, Biogot), macrophage colony stimulating factor (M-CSF) (1:100, Biogot), and E-cadherin (1:200; Abcam, Cambridge, MA, USA) as the primary antibody at 4°C overnight. After washing in PBS 3 times, the cell preparations were incubated with DyLight 488 (Green)/594 (Red)-labeled secondary antibodies (Sigma-Aldrich) for 1 h at room temperature. After washing them with PBS, the cell preparations were dropped in appropriate acacia and covered with a slide. Immunocytochemical studies were semiquantitatively or quantitatively assessed by 2 independent investigators in a blinded manner.

Flow cytometry analysis

Cells treated with AA and/or SSB were seeded for 24 h and then were collected by centrifugation. Resuspended cells were incubated with Annexin V-FITC and propidium iodide (PI) at room temperature for 5 min in the dark. Analysis of Annexin V-FITC binding by flow cytometery (Ex = 488 nm; Em = 530 nm) was accomplished using FITC signal detector and PI staining by the phycoerythrin emission signal detector.

ELISA assay

Cells treated with AA and/or SSB were seeded for 24 h, and the culture supernatant fluid was collected. Avidin-biotin-complex–enzyme-linked immunoabsorbent assay (ABC-ELISA) was used according to the manufacturer's protocol to determine MIF levels. ELISA kits were purchased from Xitang Biotechnology (Shanghai, China). All experiments were repeated at least 3 times.

LDH activity assay

Cell culture supernatant fluid was collected and LDH activities were measured by an autobiochemistry instrument (Hitachi 7600-020, Tokyo).

Reverse Transcriptase–PCR

Total RNA was extracted from NRK-52E cells using TRIzol reagent (Invitrogen), reverse-transcribed to cDNA templates using a ReverTra Ace qPCR RT Kit (Toyobo, Osaka). Quantitative RT-PCR was performed using a SYBR Green Realtime PCR Master Mix Plus (Toyobo). Quality was analyzed on agarose gels, and quantities were measured using Varioskan Flash (Thermo Fisher Scientific, Waltham, MA, USA). Sequence-specific primers of Col1a1, Col3a1, TP53, c-Myc, ZO-1, E-cadherin, vimentin, BMP-7, MMP-2, TIMP-2, MCP-1, M-CSF, and α-SMA, all listed in Table 1, were synthesized by Invitrogen, and β-actin was used as an endogenous reference gene. Samples were analyzed in triplicate. The melting curve was examined to verify that a single product was amplified. For quantitative analysis, all samples were analyzed using the $\Delta\Delta$CT value method.

Western blotting analysis

Whole proteins from NRK-52E cells were collected and protein concentrations were determined using a bicinchoninic acid protein assay kit (Beyotime Biotechnology). Whole proteins (20 μg) from each sample were separated by SDS-PAGE and transferred to a polyvinylidene difluoride membrane (Solarbio, Beijing, China). After treatment with 5% skim milk at 4°C overnight, membranes were incubated with various antibodies for 1 h and then incubated with the appropriate horseradish peroxidase–conjugated secondary antibody (Beyotime Biotechnology). Bound antibodies were visualized using chemiluminescence detection on autoradiographic film. Primary antibodies were as follows: polyclonal anti-bcl-2 (1:400, Beyotime Biotechnology), bax (1:400, Beyotime Biotechnology), NF-κB p65 (1:500; Cell Signaling Technology, Beverly, MA, USA), p53 (1:500, Biogot Technology), and c-Myc (1:500, Biogot Technology). Quantification was performed by measuring the intensity of signals using Image-Pro Plus (version 6.0) and normalized to that for the GAPDH (1:10000, Cell Signaling Technology) or β-actin antibody (1:3000, Biogot Technology).

Table 1. Real-time RT-PCR primers in this study for analysis

Gene	Sequence (5′→3′)	GenBank accession	Product size (bp)
Col1a1	GATCCTGCCGATGTCGCTAT (F) GGAGGTCTTGGTGGTTTTGTATTC (R)	NM_053304.1	276
Col3a1	AAGGCTGAAGGAAATAG (F) AATGTCATAGGGTGCGATA (R)	NM_032085.1	147
MMP-2	CGGTTTATTTGGCGGACAG (F) TGGTCAGTGGCTTGGGGTAT (R)	NM_031054.2	202
TIMP-2	GTGAGCGAGAAGGAGGTGGAT (F) CTGGGTGATGCTAAGCGTGTC (R)	NM_021989.2	273
ZO-1	AACAGAGCCGAGCAGTTAGCC (F) CAACATCAGCAATCGGTCCA (R)	NM_001106266.1	238
E-cadherin	GTGCCACCACCAAAGATA (F) GGCTGAGACAACCCTAAT (R)	NM_031334.1	195
α-SMA	GGCATCCACGAAACCACCT (F) CCGCCGATCCAGACAGAAT (R)	NM_031004.2	212
BMP-7	GTGGTCAACCCTCGGCACA (F) GGCGTCTTGGAGCGATTCTG (R)	NM_001191856.1	215
vimentin	TGACCGCTTCGCCAACTAC (F) CGCAACTCCCTCATCTCCTC (R)	NM_031140.1	141
c-Myc	CCCACCACCAGCAGCGACTC (F) GGGCTGTGAGGAGGTTTGCTGT (R)	NM_012603.2	146
TP53	TCACCATCATCACACTGGAAGACTC (F) TTGGGCAGTGCTCGCTTAGT (R)	XM_003749209.1	175
MCP-1	TGTCCCAAAGAAGCTGTAGTATTTGT (F) AGGTGGTTGTGGAAAAGAGAGTG (R)	NM_031530.1	232
M-CSF	TCTTCAATGGGCACTAACTGG (F) AAACTTCCTTTCCTGGGTCAA (R)	NM_023981.4	81
β-actin	CCCATCTATGAGGGTTACGC (F) TTTAATGTCACGCACGATTTC (R)	NM_031144.2	150

Statistical analyses

Data are presented as the mean ± S.E.M. All statistical analyses were performed using a Statistical Package for Social Sciences (version 16.0). A two-sided Student's *t*-test was used to analyze differences between the two groups. One-way analysis of variance was used when more than two groups were present. A *P*-value of < 0.05 was considered statistically significant.

Results

Apoptosis and feedback proliferation occurs in RTECs after AA injury

Evidence from phase contrast microscope showed that the injury of rat NRK-52E cells induced by AA was aggravated significantly, and cell number decreased (Fig. 2A). The viability of NRK-52E cells that were incubated for 24 h gradually decreased when the dose of AA gradually increased in a dose-dependent manner ($r = 0.817$, $P = 0.047$, Fig. 2B). In the same circumstances of drug concentration, the cell viability also decreased dramatically along with the elongation of culture time, but the correlation was poor ($r = 0.877$, $P = 0.123$).

AA at different concentrations caused different types of injury. As shown in Fig. 2C, Hoechst 33258 staining revealed that AA induced apoptosis with nuclear chromatin condensation and fragmentation as well as cell shrinkage and the formation of apoptotic bodies. In addition, AA induced cellular apoptosis at lower concentrations (1, 10 μg/ml), whereas the higher concentrates (100 μg/ml) of AA induced cell necrosis. Furthermore, injury was aggravated as cultured time lengthened. In the process of injury, enhanced expression of bcl-2 and decreased expression of bax were observed in AA-treated cells (Fig. 2D), revealing that cell apoptosis induced by AA is partly mediated by the mitochondrial pathway. However, interestingly, the mRNA expression of TP53 and c-Myc genes in NRK-52E cells was markedly increased (Fig. 2E), especially when the concentration of AA was 10 μg/ml. Elevated mRNA expression of c-Myc was considered to be related to cell proliferation

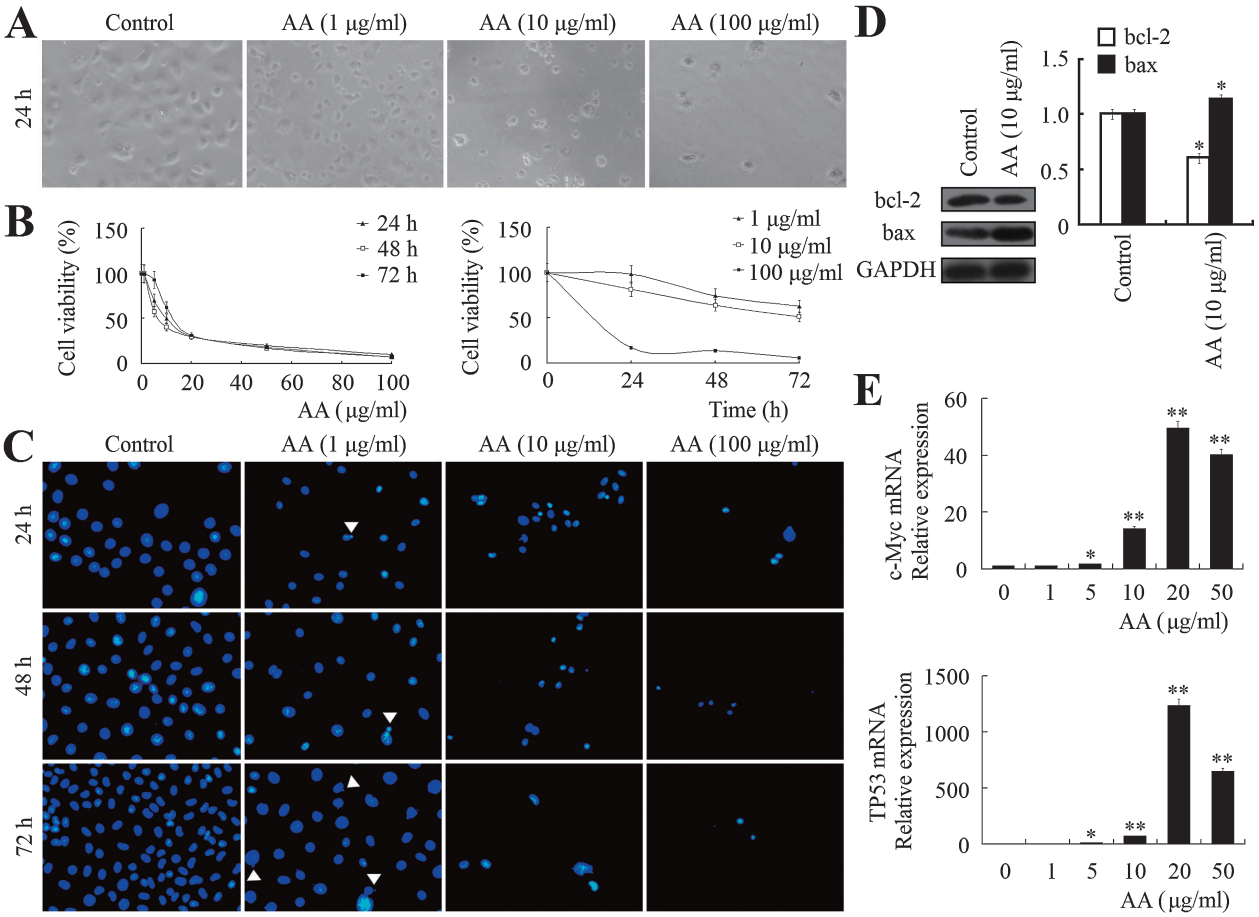


Fig. 2. AA induced renal tubular epithelial cells injury. A) Morphological change of NRK-52E cells was observed with inverted/phase contrast microscopy (× 200; Olympus, Tokyo). In response to AA, tubular epithelial cells showed obvious injury, and the cell number markedly decreased. B) Viability of NRK-52E cells were measured by WST-1 assay. The spectrophotometric analysis was determined using a Thermo Scientific Varioskan Flash (Thermo Scientific). C) Apoptosis and necrosis of NRK-52E cells were determined by Hoechst 33258 staining (× 200). The cells were then observed using a DM4000 B LED Microscope (Leica). White arrows indicated cellular apoptosis. D) Western blotting analysis indicated enhanced expression of bcl-2 and bax, suggesting that the mitochondrial pathway is involved in cell apoptosis. E) Gene expression of TP53 and c-Myc were analyzed by real-time RT-PCR using an Applied Biosystems 7500 (Life Technologies, Grand Island, NY, USA). Data are presented as the mean ± S.E.M. from independent experiments. *$P < 0.05$, **$P < 0.01$, compared with the control.

(27). As a tumor suppressor protein, p53 encoded by the TP53 gene plays a role in apoptosis, genomic stability, and inhibition of angiogenesis. However, mutations that deactivate p53 usually occur in AA-treated RTECs, and loss of regulation of cell growth, apoptosis and DNA repair. Thus, TP53 gene is transformed into an oncogene and increases the ability of cell proliferation (28). In addition, evidence from western blotting also showed AA increased the protein expression of p53 and c-Myc (Fig. 3D). These results suggested that AA at lower concentrations (< 10 μg/ml) induced apoptosis, accompanied by RTECs proliferation. The proliferation of RTECs may be through a feedback manner in order to adapt to injury to the micro-environment.

SSB induced cellular early apoptosis and inhibited proliferation

As mentioned in the previous section, in injured micro-environments, apoptosis and feedback proliferation occurs in AA-treated RTECs. A previous study showed that SSB could induce apoptosis of hepatoma cells (29). However, whether SSB shows the same effect on AA-induced RTECs injury remains unknown. Thus, cell viability of AA (10 μg/ml) in combination with SSB (10, 100, 1000 μg/ml) was determined by the WST-1 method, and cytotoxicity was detected by determining the activity of lactate dehydrogenase (LDH) in culture medium, and the apoptotic cells were examined by flow cytometry to detect labeled Annexin V-FITC/PI (Fig. 3). Our results showed that the viability of RTECs was not

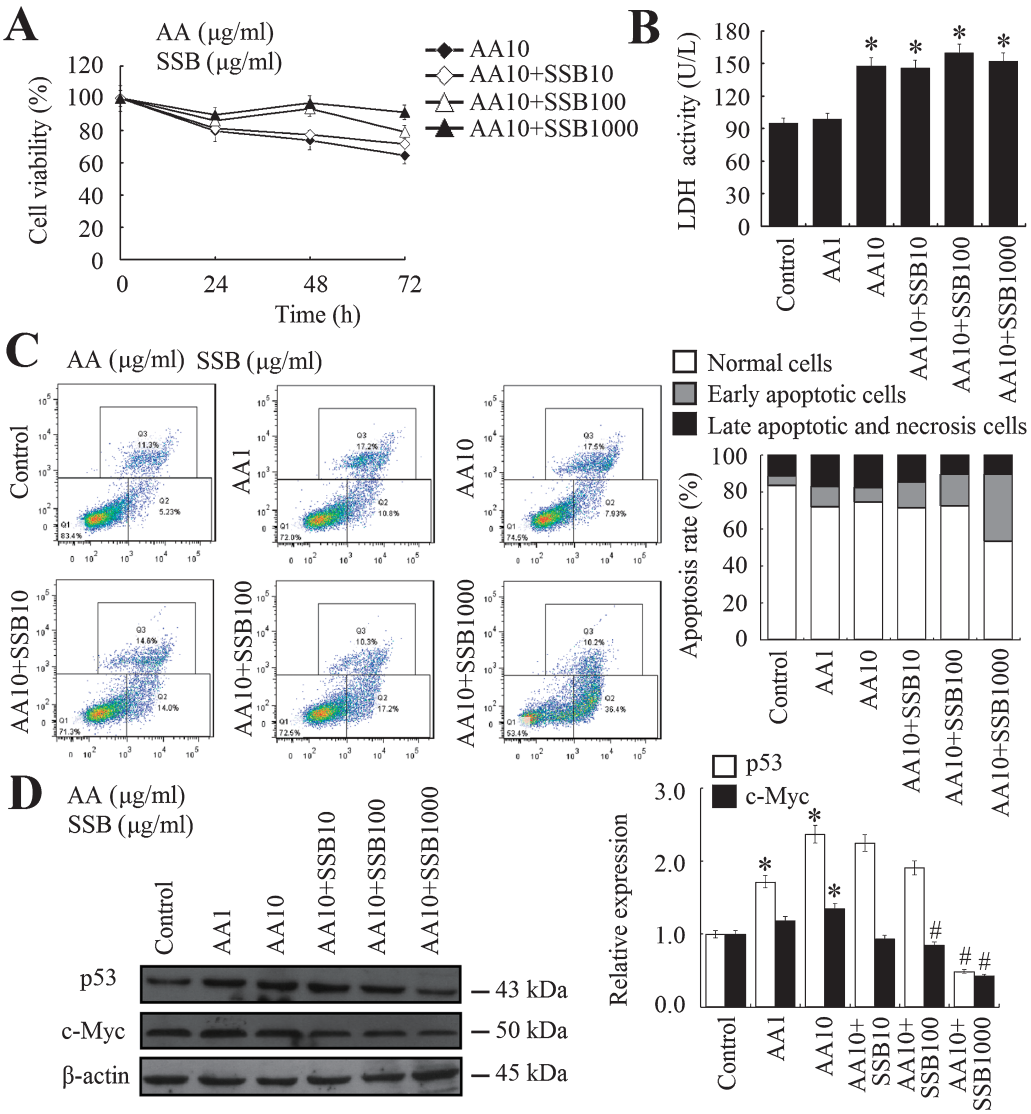


Fig. 3. SSB induced cellular apoptosis and inhibited proliferation. A) Viability of NRK-52E cells were measured by WST-1 assay. B) AA increased LDH activity but was not decreased by SSB treatment. C) Late apoptotic and necrotic cells determined by flow cytometery were significantly increased after AA injury. SSB treatment increased early apoptotic cells, not late apoptotic and necrotic cells. D) Western blotting demonstrated that AA increased protein expression of p53 and c-Myc, but was inhibited by SSB. *$P < 0.05$, compared with the control; #$P < 0.05$, compared with the AA10 group.

markedly decreased after SSB treatment, and SSB did not decrease AA-induced injury. In fact, SSB concentration-dependently increased early apoptotic cells and decreased late apoptotic and necrotic cells. Moreover, AA-induced up-regulated expression of p53 and c-Myc was suppressed by SSB. These results suggest that in vitro SSB induced early apoptosis and inhibited abnormal proliferation of RTECs.

SSB decreases ECM accumulation in AA-treated NRK-52E cells

Extensive accumulation of ECM constituents, particularly the presence of collagenous fibers, in the cortical interstitium is directly correlated to progression of renal disease. In fibrotic kidneys, the widened interstitial spaces fill with fibrillar material consisting of predominantly type I and III collagens (30). Thus, we examined the mRNA and protein expression of type I and III collagens by real-time RT-PCR and immunofluorescence staining (Fig. 4). In cultured NRK-52E cells, AA

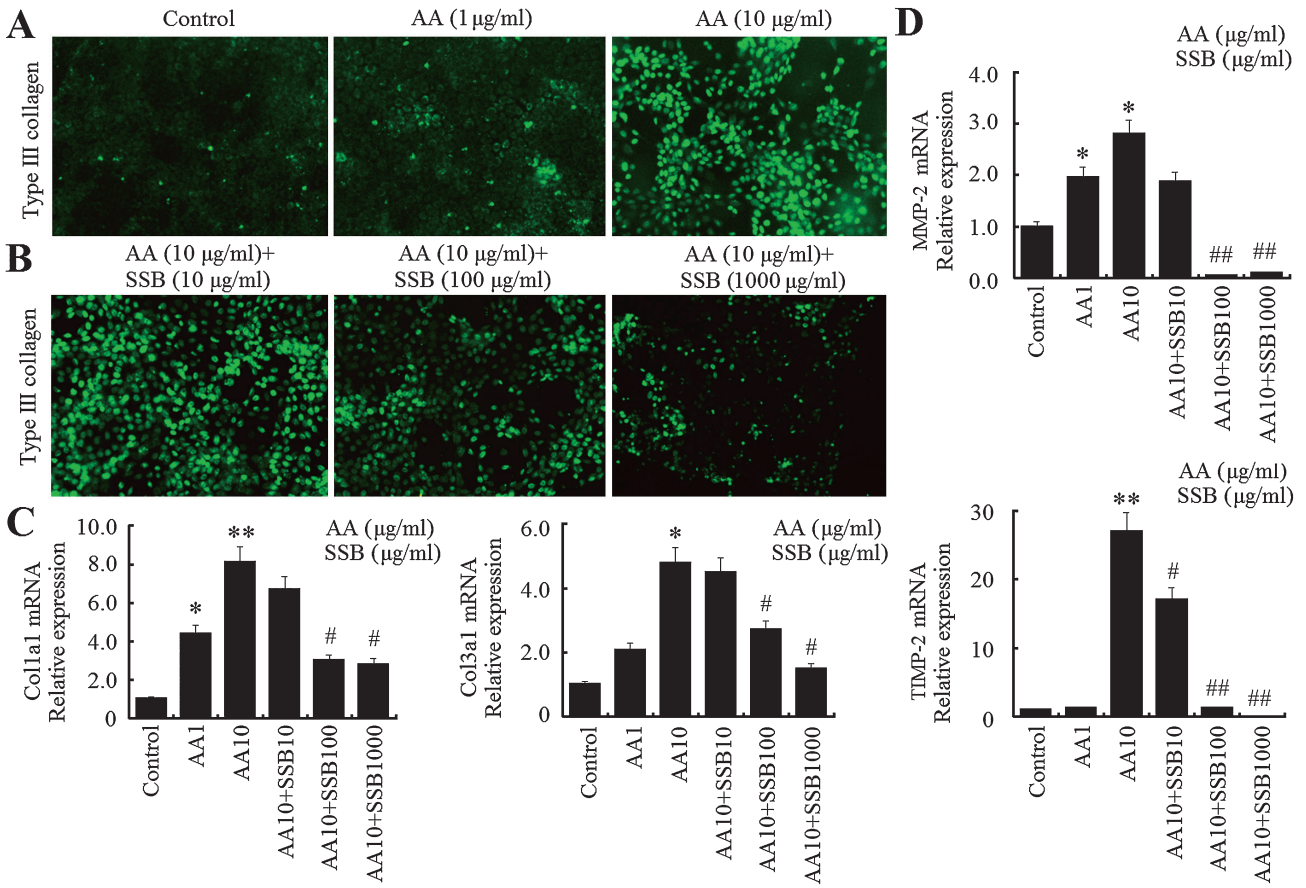


Fig. 4. SSB decreased ECM accumulation in AA-treated NRK-52E cells. A) Immunofluorescence staining indicated up-regulated expression of type III collagen in NRK-52E cells after AA injury (× 200). B) SSB treatment down-regulated expression of type III collagen in AA-treated cells. C) Gene expression of Col1a1 and Col3a1 in NRK-52E cells with AA with or without SSB. D) Gene expression of MMP-2 and TIMP-2 in NRK-52E cells with AA with or without SSB. $^{*}P < 0.05$, $^{**}P < 0.01$, compared with the control; $^{\#}P < 0.05$, $^{\#\#}P < 0.01$, compared with the AA10 group.

increased the expression of type I and III collagens. In addition, up-regulated expression of matrix metalloproteinase-2 (MMP-2) and down-regulated expression of tissue inhibitor of metalloproteinase-2 (TIMP-2) were also observed, resulting in excessive accumulation of ECM. In AA-treated cells, SSB treatment at concentrations of 10 – 100 μg/ml significantly decreased the expressions of MMP-2, type I collagen, and type III collagen and increased the expression of TIMP-2. These results suggest that SSB exerts an anti-fibrotic effect in AA-treated RTECs.

SSB inhibits AA-induced EMT in NRK-52E cells

EMT is a biologic process in which tubular cells lose their epithelial phenotype such as E-cadherin and zonula occluden-1 (ZO-1), and acquire new characteristic features of mesenchymal proteins including α-smooth muscle actin (α-SMA) and vimentin (31). As shown in Fig. 5, in cultured NRK-52E cells, AA (1, 10 μg/ml) decreased the expression of E-cadherin and ZO-1 and increased the expression of α-SMA and vimentin. In addition, down-regulated expression of BMP-7, an EMT inhibitor, was also observed in AA-treated cells. These results suggested that AA induced EMT as expected. Treatment with SSB significantly inhibited the induction of EMT after AA injury and showed obviously concentration-dependent effects.

SSB decreases expression of chemokines and pro-inflammatory cytokines

In AAN, the infiltration of inflammatory cells is involved in fibrogenesis. However, in vitro, the role of the inflammatory reaction in RTECs after AA injury and the effect of SSB need to be investigated more thoroughly. Thus, we examined the synthesis and release of many chemokines and cytokines, including monocyte chemoattractant protein-1 (MCP-1/CCL2), MIF, and M-CSF. Results from immunofluorescence staining,

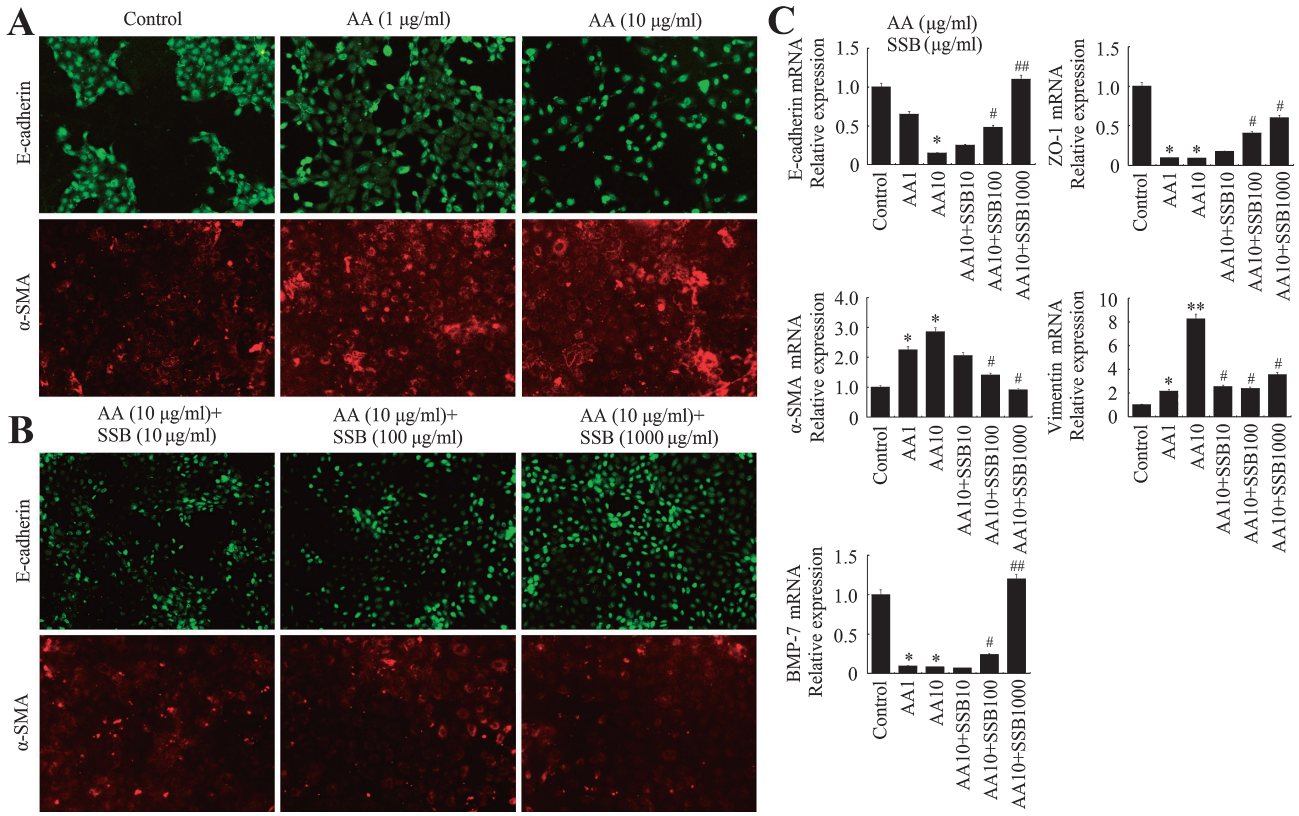


Fig. 5. SSB inhibited AA-induced EMT in NRK-52E cells. A) Immunofluorescence staining indicated that AA decreased expression of E-cadherin (an epithelial marker), and increased expression of α-SMA (a mesenchymal marker) in NRK-52E cells (× 200). B) SSB decreased expression of α-SMA and increased expression of E-cadherin in AA-treated cells, determined by immunofluorescence staining. C) Change in mRNA expression of E-cadherin, ZO-1, α-SMA, vimentin, and BMP-7 in NRK-52E cells treated with AA with or without SSB, detected by real-time RT-PCR. $^{*}P < 0.05$, $^{**}P < 0.01$, compared with the control; $^{\#}P < 0.05$, $^{\#\#}P < 0.01$, compared with the AA10 group.

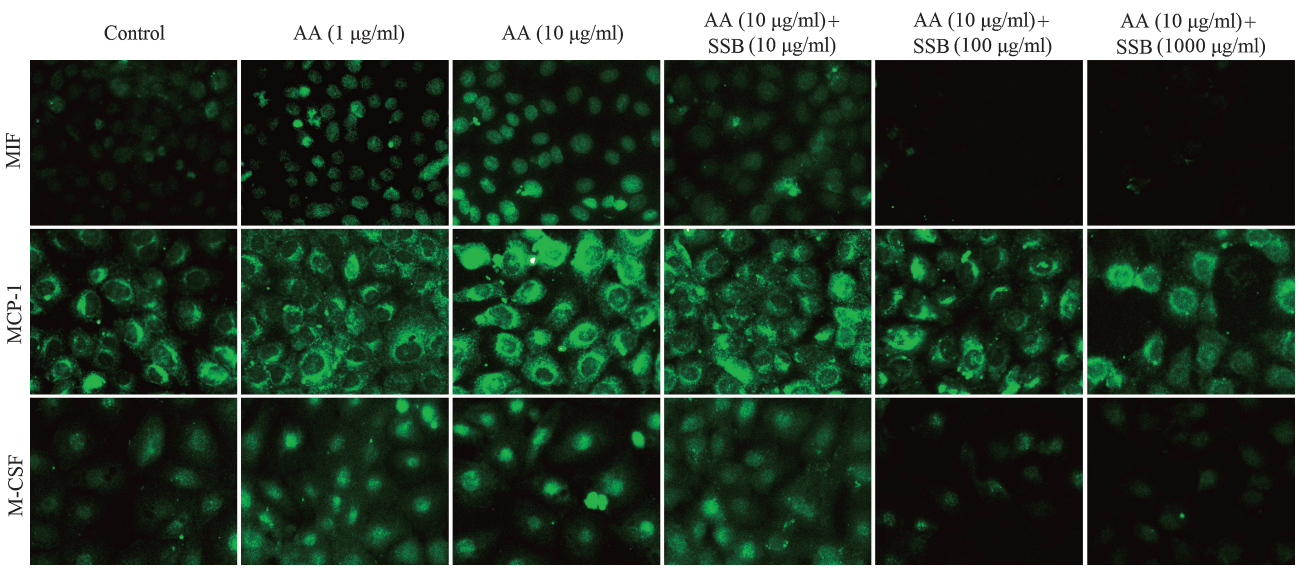


Fig. 6. Expression of MIF, MCP-1, and M-CSF in NRK-52E cells with AA with or without SSB. Immunofluorescence staining indicated down-regulated expression of MIF, MCP-1, and M-CSF in NRK-52E cells treated with AA, and up-regulated expression in cells treated with AA and SSB (× 400).

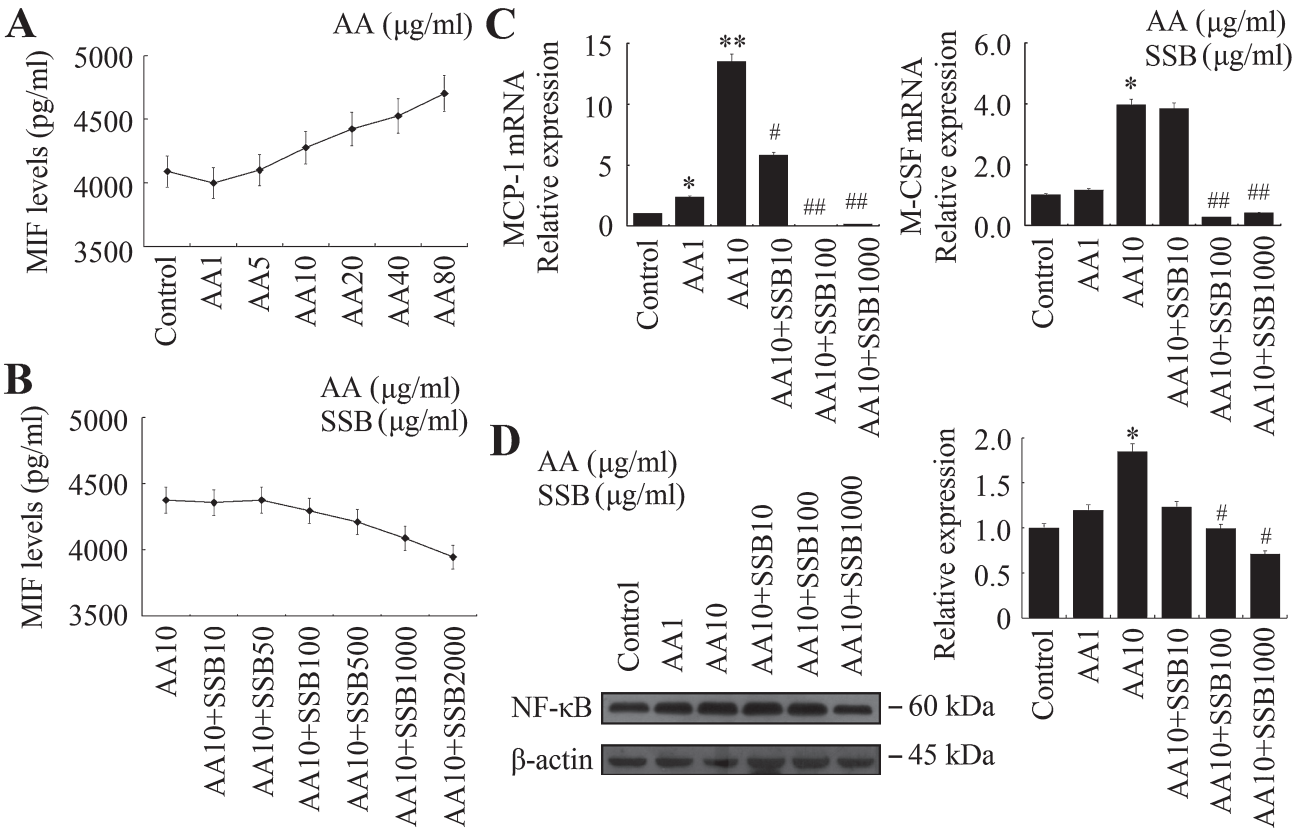


Fig. 7. SSB decreased expression of chemokines and pro-inflammatory cytokines. A) ELISA demonstrated that AA increased MIF levels in a concentration-dependent manner. B) SSB decreased MIF levels in AA-treated cells. C) Gene expression of MCP-1 and M-CSF in NRK-52E cells with AA with or without SSB. D) AA increased protein expression of NF-*κ*B p65 and SSB treatment decreased AA-induced over-expression of NF-*κ*B p65. $^{*}P < 0.05$, $^{**}P < 0.01$, compared with the control; $^{\#}P < 0.05$, $^{\#\#}P < 0.01$, compared with the AA10 group.

ELISA, and real-time RT-PCR show that AA increased the expression of MIF, MCP-1, and M-CSF in a concentration-dependent manner (Figs. 6 and 7), but enhanced expression of these factors was suppressed by SSB treatment. These results suggest that AA induces an inflammatory response and macrophages might be involved in this process and renal fibrogenesis. Treatment with SSB can inhibit the macrophage-mediated inflammatory response.

AA activated NF-κB signaling but was inhibited by SSB

NF-*κ*B is a transcription factor that regulates the gene expression of chemokines and cytokines, which contribute to the recruitment of inflammatory cells in the kidney tissue (32). As shown in Fig. 7, AA increased NF-*κ*B p65 activity in cultured NRK-52E cells compared with the control, as assessed by western blotting. However, increased expression of NF-*κ*B p65 was inhibited by SSB treatment. Thus, SSB may inhibit the synthesis of inflammatory factors by blocking the NF-*κ*B signaling pathway.

Discussion

Previous pharmacological studies revealed that SSB possess significant bioactivities on anti-inflammation, anti-tumor, and anti-viral infection (16 – 18). In this study, we identified the anti-fibrosis effect of SSB in RTECs after AA injury.

Firstly, we examined AA-induced injury of the cultured NRK-52E cells. Our results showed that AA not only significantly decreased the viability and number of NRK-52E cells, but also increased the apoptosis rate, accompanied by up-regulated expression of bcl-2 and down-regulated expression of bax. These suggest that AA induces mitochondrial pathway–mediated cellular apoptosis. It is believed now that the reasons for RTEC apoptosis induced by AA exposure include intracellular calcium ion concentration (33, 34), the formation of specific AA-DNA adducts (35), and cell cycle arrest (9). The damage of AA to DNA or protein results in cellular apoptosis via p53-mediated signaling (36). AA induced subsequent activation of p53, and p53 inhibition or

p53 knock-down with small interfering RNA attenuated AA-induced RTEC apoptosis. Our study also demonstrated that AA significantly increased the mRNA and protein expression of p53. Moreover, the mRNA and protein expression of c-Myc was also increased in AA-treated NK-52E cells. Enhanced expression of c-Myc is involved in RTEC proliferation. We believed that there exist a feedback mechanism for cell proliferation, and the proliferation of RTECs is needed to adapt to injury within the micro-environment. However, the abnormal proliferation may lead to a bad denouement, including phenotypic transformation and ECM deposition. Treatment with SSB decreased the expression of p53 and c-Myc and increased apoptotic RTECs, especially for early apoptotic cells. Thus, SSB exerts inhibition on RTEC proliferation, accompanied by the induction of cellular apoptosis.

In vivo evidence from many studies showed that persistent injury of AA results in renal tubulointerstitial fibrosis (4, 9). In cultured RTECs, we observed that AA increased the expression of type I and III collagens. Moreover, AA increased MMP-2 expression and decreased TIMP-2 expression. MMP-2, which is regulated by TIMP-2, is a member of the matrix metalloproteinase family that is involved in the breakdown of ECM in normal physiological processes such as embryonic development and tissue remodeling (37). In fibrogenesis, up-regulation of MMP-2 expression and down-regulation of TIMP-2 expression may be responsible for a decrease in the degradation of ECM and increase in its synthesis, resulting in extensive accumulation of ECM constituents. Thus, these results suggested that AA promoted ECM production in vitro. ECM components in kidney are synthesized and secreted by myofibroblast cells, which originate from activated resident fibroblast and epithelial cells undergoing EMT (38). EMT may be an adaptive response of epithelial cells after injury and is increasingly recognized as an integral part of renal fibrogenesis (31). In this study, AA increased the expression of mesenchymal genes α-SMA and vimentin and decreased the expression of epithelial markers E-cadherin and ZO-1 in cultured RTECs. In addition, decreased expression of the EMT inhibitor BMP-7 was observed in AA-treated RTECs. Thus, AA promotes the transition of RTECs to ECM-producing cells. Compared to epithelial cells, ECM-producing cells (mesenchymal cells) possess stronger ability to adapt to injured micro-environment. This phenotypic transition may be an outcome of abnormal proliferation of RTECs. Treatment with SSB abolished the induction of EMT and reduced the deposition of ECM components, although the expression levels of all of the molecules did not return to normal levels. Thus, SSB exerts marked anti-renal fibrosis effects.

In fibrogenesis, the macrophage-mediated inflammatory reaction plays an important role. Activated macrophages during an inflammatory reaction can release a variety of cytokines, such as TGF-β1 and platelet-derived growth factor (PDGF) (39), to exert profibrogenic effects. In AA-treated RTECs, injury did not induce the infiltration of inflammation cells, but could regulate the synthesis and release of inflammatory factors. In this study, the expression levels of MIF, MCP-1, and M-CSF were significantly increased in RTECs after AA injury. MIF is recognized as an important immunoregulatory molecule expressed in various kinds of cells, including mononuclear macrophages and epithelial cells (13, 14) and arrests random immune cell movement (40). MIF participates in the immune and inflammatory responses of many tissues and organs. MCP-1 is primarily secreted by monocytes, macrophages, and epithelial cells and exhibits a chemotactic activity for monocytes (41). M-CSF is a hematopoietic growth factor that is involved in the proliferation, differentiation, and survival of monocytes and macrophages. Thus, change in expression of MIF, MCP-1, and M-CSF reflects the activity and function of monocytes and macrophages. Increased expression of these factors in our study demonstrates that activated macrophages are involved in the AA-induced inflammatory reaction. We found that treatment with SSB could decrease the expression levels of MIF, MCP-1, and M-CSF and thus inhibit the monocyte- and macrophage-mediated inflammatory reaction.

In addition, our study also showed that SSB could decrease the activity of NF-κB p65. The NF-κB signaling pathway is found in almost all animal cell types and plays a key role in regulating the immune response to infection. Activation of NF-κB signaling induces inflammation-related gene transcription, including MIF, MCP-1, and M-CSF (13 – 15). Thus, enhanced expression of MIF, MCP-1, and M-CSF in AA-treated RTECs is associated with up-regulated activity of NF-κB signaling. SSB inhibited the activation of NF-κB signaling, down-regulated expression of MIF, MCP-1, and M-CSF, and resulted in reduction of monocyte and the macrophage-mediated inflammatory reaction.

In conclusion, our in vitro experiments clarified the injury and fibrosis mechanisms of AA on RTECs and preliminarily identified the anti-fibrosis effect of SSB. Our results suggest that SSB at certain concentration can induce cellular apoptosis, inhibit proliferation, inhibit the induction of EMT, and ECM accumulation. Moreover, SSB can inhibit the synthesis of monocyte- and macrophage-mediated inflammatory factors by the NF-κB signaling pathway. However, due to the

complexity of the chemical constituents of SSB, the underlying molecular mechanisms of SSB triggering the anti-fibrogenic response still need to be further studied in vivo. In addition, the dosage and safety of SSB needs to be clarified.

Acknowledgments

This study was sponsored by Zhejiang Extremely Key Subject of Surgery and Youth Talent Plan of First Affiliated Hospital of Wenzhou Medical University and supported by the Wenzhou Municipal Science and Technology Plan Project (Grant No. Y20110028 and Y20110072). This project was also supported by the Natural Science Foundation of Zhejiang province, China (Grant No. LQ12H050001 and LY12H050004).

Conflicts of Interest

The authors declare that they have no competing interests.

References

1 Arlt VM, Stiborova M, Schmeiser HH. Aristolochic acid as a probable human cancer hazard in herbal remedies: a review. Mutagenesis. 2002;17:265–277.
2 Cosyns JP. Aristolochic acid and “Chinese herbs nephropathy”: a review of the evidence to date. Drug Saf. 2003;26:33–48.
3 Depierreux M, Van Damme B, Vanden Houte K, Vanherweghem JL. Pathologic aspects of a newly described nephropathy related to the prolonged use of Chinese herbs. Am J Kidney Dis. 1994;24:172–180.
4 Chen W, Chen Y, Li A. [The clinical and pathological manifestations of aristolochic acid nephropathy--the report of 58 cases]. Zhonghua Yi Xue Za Zhi. 2001;81:1101–1105. (text in Chinese)
5 Debelle FD, Vanherweghem JL, Nortier JL. Aristolochic acid nephropathy: a worldwide problem. Kidney Int. 2008;74: 158–169.
6 Tanaka A, Shinkai S, Kasuno K, Maeda K, Murata M, Seta K, et al. [Chinese herbs nephropathy in the Kansai area: a warning report]. Nihon Jinzo Gakkai Shi. 1997;39:438–440. (text in Japanese)
7 Baudoux TE, Pozdzik AA, Arlt VM, De Prez EG, Antoine MH, Quellard N, et al. Probenecid prevents acute tubular necrosis in a mouse model of aristolochic acid nephropathy. Kidney Int. 2012;82:1105–1113.
8 Docherty NG, O’Sullivan OE, Healy DA, Fitzpatrick JM, Watson RW. Evidence that inhibition of tubular cell apoptosis protects against renal damage and development of fibrosis following ureteric obstruction. Am J Physiol Renal Physiol. 2006;290:F4–F13.
9 Yang L, Besschetnova TY, Brooks CR, Shah JV, Bonventre JV. Epithelial cell cycle arrest in G2/M mediates kidney fibrosis after injury. Nat Med. 2010;16:535–543.
10 Zeisberg M, Neilson EG. Biomarkers for epithelial-mesenchymal transitions. J Clin Invest. 2009;119:1429–1437.
11 Wang Z, Zhao J, Zhang J, Wei J, Huang Y. Protective effect of BMP-7 against aristolochic acid-induced renal tubular epithelial cell injury. Toxicol Lett. 2010;198:348–357.
12 Zeisberg M, Hanai J, Sugimoto H, Mammoto T, Charytan D, Strutz F, et al. BMP-7 counteracts TGF-beta1-induced epithelial-to-mesenchymal transition and reverses chronic renal injury. Nat Med. 2003;9:964–968.
13 Rice EK, Tesch GH, Cao Z, Cooper ME, Metz CN, Bucala R, et al. Induction of MIF synthesis and secretion by tubular epithelial cells: a novel action of angiotensin II. Kidney Int. 2003;63:1265–1275.
14 Chen L, Yang G, Zhang X, Wu J, Gu Q, Wei M, et al. Induction of MIF expression by oxidized LDL via activation of NF-kappaB in vascular smooth muscle cells. Atherosclerosis. 2009;207: 428–433.
15 Sanchez-Lopez E, Rayego S, Rodrigues-Diez R, Rodriguez JS, Rodriguez-Vita J, Carvajal G, et al. CTGF promotes inflammatory cell infiltration of the renal interstitium by activating NF-kappaB. J Am Soc Nephrol. 2009;20:1513–1526.
16 Cao SP, Liu LF, Wang Q. [Determination of triterpene delta-amyrone in Sedum sarmentosum]. Zhongguo Zhong Yao Za Zhi. 2006;31:41–42,50. (text in Chinese)
17 Heo BG, Park YS, Chon SU, Lee SY, Cho JY, Gorinstein S. Antioxidant activity and cytotoxicity of methanol extracts from aerial parts of Korean salad plants. Biofactors. 2007;30:79–89.
18 Jung HJ, Kang HJ, Song YS, Park EH, Kim YM, Lim CJ. Anti-inflammatory, anti-angiogenic and anti-nociceptive activities of Sedum sarmentosum extract. J Ethnopharmacol. 2008;116: 138–143.
19 Morikawa T, Zhang Y, Nakamura S, Matsuda H, Muraoka O, Yoshikawa M. Bioactive constituents from Chinese natural medicines. XXII. Absolute structures of new megastigmane glycosides, sedumosides E1, E2, E3, F1, F2, and G, from Sedum sarmentosum (Crassulaceae). Chem Pharm Bull (Tokyo). 2007; 55:435–441.
20 Ninomiya K, Morikawa T, Zhang Y, Nakamura S, Matsuda H, Muraoka O, et al. Bioactive constituents from Chinese natural medicines. XXIII. Absolute structures of new megastigmane glycosides, sedumosides A(4), A(5), A(6), H, and I, and hepatoprotective megastigmanes from Sedum sarmentosum. Chem Pharm Bull (Tokyo). 2007;55:1185–1191.
21 Oh H, Kang DG, Kwon JW, Kwon TO, Lee SY, Lee DB, et al. Isolation of angiotensin converting enzyme (ACE) inhibitory flavonoids from Sedum sarmentosum. Biol Pharm Bull. 2004; 27:2035–2037.
22 Sun J, Sun G, Meng X, Wang H, Luo Y, Qin M, et al. Isorhamnetin protects against doxorubicin-induced cardiotoxicity in vivo and in vitro. PLoS One. 2013;8:e64526.
23 Johari J, Kianmehr A, Mustafa MR, Abubakar S, Zandi K. Antiviral activity of Baicalein and Quercetin against the Japanese encephalitis virus. Int J Mol Sci. 2012;13:16785–16795.
24 Wang G, Song L, Wang H, Xing N. Quercetin synergizes with 2-methoxyestradiol inhibiting cell growth and inducing apoptosis in human prostate cancer cells. Oncol Rep. 2013;30:357–363.
25 Youn H, Jeong JC, Jeong YS, Kim EJ, Um SJ. Quercetin potentiates apoptosis by inhibiting nuclear factor-kappaB signaling in H460 lung cancer cells. Biol Pharm Bull. 2013;36: 944–951.
26 Mahmoud MF, Hassan NA, El Bassossy HM, Fahmy A. Quercetin protects against diabetes-induced exaggerated vasoconstriction in rats: effect on low grade inflammation. PLoS One. 2013;8:e63784.
27 Junk DJ, Cipriano R, Stampfer M, Jackson MW. Constitutive CCND1/CDK2 activity substitutes for p53 loss, or MYC or

oncogenic RAS expression in the transformation of human mammary epithelial cells. PLoS One. 2013;8:e53776.
28 Arlt VM, Schmeiser HH, Pfeifer GP. Sequence-specific detection of aristolochic acid-DNA adducts in the human p53 gene by terminal transferase-dependent PCR. Carcinogenesis. 2001;22: 133–140.
29 Huang D, Zhang W, Wu J. Antitumor activity of the aqueous extract from Sedum sarmentosum Bunge in vitro. Cancer Biother Radiopharm. 2010;25:81–88.
30 Kuncio GS, Neilson EG, Haverty T. Mechanisms of tubulointerstitial fibrosis. Kidney Int. 1991;39:550–556.
31 Liu Y. New insights into epithelial-mesenchymal transition in kidney fibrosis. J Am Soc Nephrol. 2009;21:212–222.
32 Guijarro C, Egido J. Transcription factor-kappa B (NF-kappa B) and renal disease. Kidney Int. 2001;59:415–424.
33 Balachandran P, Wei F, Lin RC, Khan IA, Pasco DS. Structure activity relationships of aristolochic acid analogues: toxicity in cultured renal epithelial cells. Kidney Int. 2005;67:1797–1805.
34 Hsin YH, Cheng CH, Tzen JT, Wu MJ, Shu KH, Chen HC. Effect of aristolochic acid on intracellular calcium concentration and its links with apoptosis in renal tubular cells. Apoptosis. 2006; 11:2167–2177.
35 Lebeau C, Arlt VM, Schmeiser HH, Boom A, Verroust PJ, Devuyst O, et al. Aristolochic acid impedes endocytosis and induces DNA adducts in proximal tubule cells. Kidney Int. 2001;60:1332–1342.
36 Zhou L, Fu P, Huang XR, Liu F, Lai KN, Lan HY. Activation of p53 promotes renal injury in acute aristolochic acid nephropathy. J Am Soc Nephrol. 2009;21:31–41.
37 Ban CR, Twigg SM. Fibrosis in diabetes complications: pathogenic mechanisms and circulating and urinary markers. Vasc Health Risk Manag. 2008;4:575–596.
38 Meran S, Steadman R. Fibroblasts and myofibroblasts in renal fibrosis. Int J Exp Pathol. 2011;92:158–167.
39 Bonner JC, Osornio-Vargas AR, Badgett A, Brody AR. Differential proliferation of rat lung fibroblasts induced by the platelet-derived growth factor-AA, -AB, and -BB isoforms secreted by rat alveolar macrophages. Am J Respir Cell Mol Biol. 1991;5:539–547.
40 Zernecke A, Bernhagen J, Weber C. Macrophage migration inhibitory factor in cardiovascular disease. Circulation. 2008; 117:1594–1602.
41 Lundien MC, Mohammed KA, Nasreen N, Tepper RS, Hardwick JA, Sanders KL, et al. Induction of MCP-1 expression in airway epithelial cells: role of CCR2 receptor in airway epithelial injury. J Clin Immunol. 2002;22:144–152.